

Minimising Power System Losses and Improving Voltage Profile Through Optimal PV Penetration

Hesain M. Alfrd¹, Abdolkarem Salem S. Ebshish²

¹hussein.alfared@elmergib.edu.ly, Lecturer at Electrical & Computer Dept, University of Elmergib, Libya

²asebshish@elmergib.edu.ly, Lecturer at Electrical & Computer Dept, University of Elmergib, Libya

Abstract- In recent years, there has been a growing global interest in boosting the contribution of solar energy to electrical networks. This is because it is a clean energy source with no negative environmental impact. Furthermore, the development of solar panels is increasing, and so is the price decrease. High-voltage electrical power inverter manufacturing has also advanced, allowing solar energy units to be connected to high-voltage networks. Despite these advantages, there are numerous problems. With growing worried about global warming, most countries are advocating for a cleaner alternative to present fossil fuel-based generation systems. Photovoltaic (PV) installations are becoming more popular because of their adaptability. Compared to typical generation systems, PV is placed closer to load centres. This allows injecting PV at optimal locations and sizes to reduce system losses and improve the voltage profile. This paper considers the optimal PV penetration percentage size and location placement. Simulation is performed on the IEEE 14 bus system using Neplan software. When the system is optimised, the voltage profile improves significantly while losses are reduced.

Keywords – PV penetration, minimizing power losses, improving voltage profile, optimal size and location of PV

I. INTRODUCTION

With growing concerns about global warming, there has been a surge in demand for greener alternatives. As a result, the global installation of large-scale solar has increased dramatically. According to research, solar radiation provides around 1.8×10^{11} MW of power to the earth's surface at any given time. This is sufficient to meet the global electricity demand [1]. Solar energy can be harvested in two ways: thermal and photovoltaic. However, photovoltaics is a more viable choice [2]. Furthermore, with changes to energy sector rules, several countries are projected to incorporate large-scale renewable generation into the existing system. For example, in 2015, China's total installed photovoltaic capacity was 43.18 TW. China is on track to become the world's largest installed photovoltaic generation capacity [3]. India installed 87.20 GW of solar power capacity. India aims to install 500 GW of renewable energy capacity by 2030 [4]. Nonetheless, because of the unpredictable nature of PV, integrating PV into the existing grid would have a few negative consequences for the system if not done correctly. Power losses and voltage profiles are essential indications of power quality and reliability and comparing shunt capacitors and distributed generation (DG) can help improve both [5]. Heavy loads and faults are the primary causes of voltage instability [6]. The most typical concerns include steady-state overvoltage, its effect on the voltage profile, rapid voltage fluctuations, and the impact on system losses. Voltage profile and system losses are the most essential areas of concern for firms because they affect system reliability, power outages, and financial losses to the utility [7],[8].

Furthermore, increasing PV penetration reduces the system's inertia as the power supplied by traditional generators decreases. The reduction in active power supplied to the system will have an impact on its transient stability [9]. Voltage stability is defined as a system's capacity to maintain an acceptable voltage across its components after a disturbance [10]. In this paper, the stability limits are specified at $\pm 5\%$ of the base value. Any deviation from this limit is regarded as system unstable. Most power utilities globally use $\pm 5\%$ as the actual operational voltage limit. When PV is included, the system's

voltage stability limit increases. As a result, the system's ability to transfer active power is increased. However, the size of installed PV systems must be limited. Otherwise, the PV's power output will exceed the system load, resulting in reverse power [11]. Furthermore, if the rise in PV penetration level is not regulated, the system will lose stability and surpass the utility-set limitations. Several research have been conducted to determine the optimal PV allocation. The procedure has been implemented using a variety of strategies, including analytical tools and programming optimization methods [12].

The extant research on voltage variations is limited because most studies focus on safety index limitations. A few have emphasized the significance of voltage changes for calculating DG capacity [13],[14]. However, these studies have not examined the relationship between available PV capacity and power factor [15]. Besides the level of PV penetration and PV size allocation, the power factor of PV is another important component that influences the voltage profile and system losses. When PV is integrated, the system's power factor (PF) can fall to undesirable levels ($PF > 0.85$). When PV production exceeds 10% of the system power, several studies recommend operating at a power factor greater than 0.85 (leading/lagging) [16].

This study explores the optimal position and size for photovoltaic (PV) installations on the IEEE 14 bus system. Neplan software is used to simulate the network, focusing on bus voltages and active losses to determine the optimal PV penetration size and placement for achieving the lowest losses while increasing the voltage profile.

II. CHARACTERISTICS AND MODELLING OF SOLAR PHOTOVOLTAIC CELLS SYSTEM

Photovoltaic (PV) systems convert light energy to electricity. The term "photo" comes from the Greek for "light". "Volt" is named after Alessandro Volta (1745-1827), a pioneer in the study of electricity. PV might literally imply "light-electricity" [17]. A grid-connected PV system transforms sunlight directly into alternating current (AC) electricity. The system's primary goal is to lower the amount of electricity imported from the electric utility.

Figure 1 depicts a functional schematic of the fundamental setup of a grid-connected PV system. The DC output current of the PV array I_{pv} is converted to AC and fed into the grid via an inverter. This inverter's controller executes all the key control and protection functions, including Maximum Power Point Tracking (MPPT), a protective relay, and islanding operation detection.

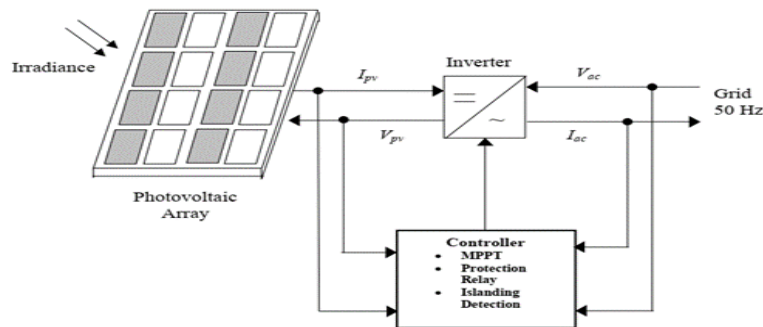


Figure 1 Basic configuration of grid-connected PV generation [18].

A. Photovoltaic cells

Semiconductors, which can be manufactured using a variety of processes, are the basic components of solar cells. These semiconductors convert solar energy directly into electricity using a process known as the photovoltaic effect.

The whole I-V curve of a cell, module, or array is specified as a continuous function for equivalent circuit models, regardless of the operating conditions under consideration. Figure 2 depicts a solar photovoltaic cell. This cell consists of a continuous current source that depends on the amount of solar radiation, a diode with a series resistance (R_s), and a parallel resistance (R_{sh}) [18].

A dark current, also known as a backward current (I_0), flows in a p-n junction when there is no solar radiation (G) from the sun. The cell produces the current I_p with a load connected when there is solar radiation. When there is no load connected, the voltage V_{pv} is the open circuit voltage that can be measured. The greatest current that a cell can produce at a specific level of solar radiation is known as the current $I_p(G)$.

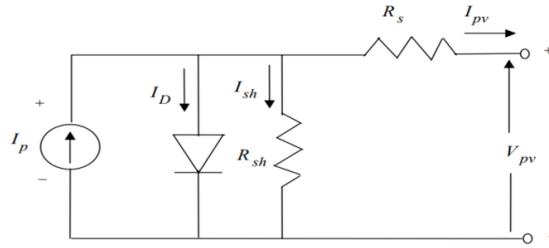


Figure 2 Solar cell equivalent model [18].

The following equation represents a PV cell:

$$\begin{aligned}
 I_{pv} &= I_p - I_D - I_{sh} \\
 &= I_p - I_o \left[e^{\frac{q(V_{pv} + R_s I_{pv})}{NkT}} - 1 \right] - \frac{V_{pv} + R_s I_{pv}}{R_{sh}}
 \end{aligned} \tag{1}$$

Where

I_p = Photocurrent [A]

V_{pv} = Terminal voltage of the cell [V]

I_D = Diode current [A]

I_o = Saturation current [A]

I_{sh} = Shunt current [A]

N = Ideality factor (a material constant)

q = Electron charge [C]

k = Boltzmann's constant (8.62×10^{-5} eV/K)

T = Junction temperature [K] (diode temperature)

R_s = Series resistance [Ω]

R_{sh} = Shunt resistance [Ω]

B. Inverter

The ability to convert the PV array's DC output into AC power to feed to the utility network is a crucial component of a grid-connected PV system. Inverters are utilised to accomplish this purpose. The two main types of inverters are thyristor-based line commutated inverters (TLCI) and pulse width modulated (PWM) voltage source inverters. Figures 3 and 4 depict these two types of inverters, respectively [19].

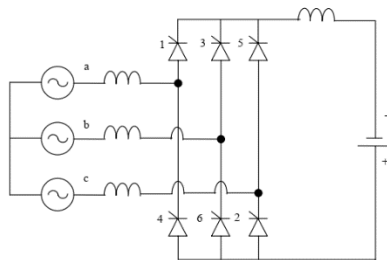


Figure 3 TLCI inverter connected PV generation [18].

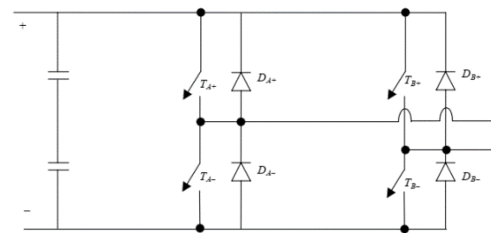


Figure 4 PWM voltage source inverter generation [18].

Many existing PV systems employ TLCI-type inverters because of their low cost, ability to handle higher power levels, and familiarity with the technology. If this inverter is directly connected to the PV array, the current drawn from it can be regulated by adjusting the firing angle. This type of inverter is often used in grid-connected PV installations.

Advancements in IGBT (Insulated Gate Bipolar Transistor) and MOSFET (Metal Oxide Semiconductor Field Effect Transistor) technology, along with quick real-time digital control, have resulted in the adoption of high-quality sinusoidal PWM voltage source inverters in PV systems.

The increased flexibility of modern inverters, combined with the usage of microprocessors, allows for easy and appropriate configuration of the inverter for a specific application. Many existing PV systems employ TLCI-type inverters due to their low cost, ability to handle higher power levels, and familiarity with the technology. If this inverter is directly connected to the PV array, the current drawn from it can be regulated by adjusting the firing angle. This type of inverter is often used in grid-connected PV installations.

Advancements in IGBT (Insulated Gate Bipolar Transistor) and MOSFET (Metal Oxide Semiconductor Field Effect Transistor) technology, along with quick real-time digital control, have resulted in the adoption of high-quality sinusoidal

PWM voltage source inverters in PV systems. The increased flexibility of modern inverters, combined with the usage of microprocessors, allows for easy and appropriate configuration of the inverter for a specific application.

In these inverters, the magnitude of the input DC voltage is practically constant, and the inverters' output voltage and frequency can be controlled. This is accomplished using Pulse Width Modulation of the inverter switches, hence the name PWM inverters.

C. Effect of Irradiance and Cell Temperature

Figures 5 and 6 depict, respectively, the impact of irradiance and cell temperature on the I_{pv} - V_{pv} characteristic curve. The maximum power production changes approximately linearly, with radiations higher than 0.75 kW/m^2 , with the irradiance, as Figure 5 illustrates. Figure 6 illustrates how the array's maximum output power drops with temperature [20].

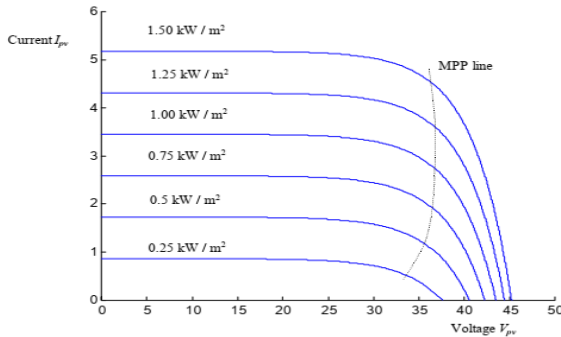


Figure 5 Effect of irradiance on the I-V characteristic at constant cell temperature generation [18].

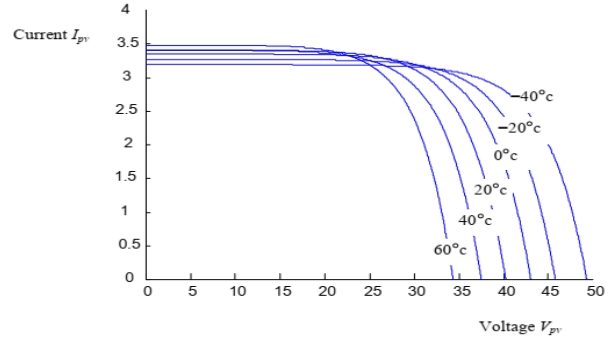


Figure 6 Effect of temperature on the I-V characteristic at constant irradiance generation [18].

D. Maximum Power Point Tracking Controller

The I_{pv} - V_{pv} characteristic of a photovoltaic cell is dependent on the operating temperature and irradiance of the cell. The maximum power point fluctuates as a result. Therefore, the PV system cannot produce its full power when a fixed voltage, fixed current, or fixed resistance load is directly connected. The PV array must always be run at its maximum power point to provide the most power possible. Thus, a controller that can monitor the maximum power point needs to be used. There are several maximum power point tracking (MPPT) techniques. All these solutions require an algorithm to specify the operating point's position relative to the greatest PowerPoint. Some of them produce just sub-optimal power output. Because PV systems must be mass-produced, an effective MPPT technology should yield great efficiency at a reasonable cost [21].

III. IMPACT OF INTEGRATION OF SOLAR PV POWER SYSTEMS ON THE VOLTAGE PROFILE

A voltage profile is a numerical representation of the voltage level at a bus of a grid under various operational situations. Measuring the voltage level can account for conditions such as no load, light load, full load, and overload. The great majority of power systems require the grid voltage to remain within a specific range.

This is due to the fact that even little fluctuations in supply voltage have an unfavourable effect on the operation of certain loads. Voltage instability may develop if the voltage profile changes significantly. Utility businesses, as well as transmission and distribution grid operators, share the goal of maintaining a healthy voltage profile, consistent grid characteristics, and reliable voltage. Grid characteristics must always remain stable, including during system updates, the incorporation of additional power units, and operations.

Changes in operating conditions may also affect the power system's loading and losses [22]. A two-port system with a short line, end voltage (V_2), transmitting end voltage (V_1), and load (P, Q) is used to show the voltage profile. Using the two-port system, we may extract ideas about system behaviour in terms of voltage and stability. Figure 7 depicts a two-part system representation.

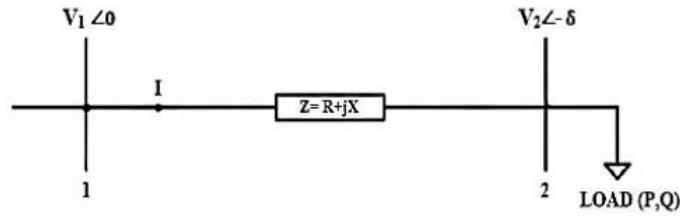


Figure 7 Two-bus power system [23].

Equation (2) is derived from the analysis of Figure 7 for the voltage relationship between bus 1 and bus 2:

$$V_1 = V_2 + IZ \tag{2}$$

Calculate the receiving bus voltage as:

$$|V_2| = |V_1| - \frac{(RP + XQ)}{|V_2|} \tag{3}$$

According to Eq. (3), under specific operating and loading conditions, bus 2's voltage magnitude and profile are expressed as |V₂|. With the third term, calculate the voltage drop can be calculated. Voltage drop is a result of the line parameters (R and X). Yet, the bus 2 is receiving the load, both active and reactive power are used, as illustrated in (4).

Voltage drops:

$$\Delta V = \frac{(RP + XQ)}{|V_2|} \tag{4}$$

The two-part system with solar photovoltaic power is depicted in Figure 8. A solar PV plant may be connected to a two-pole grid if active power with a unity power factor is added to bus 2.

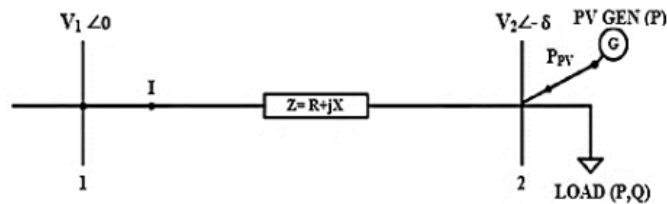


Figure 8 Two-node system with solar PV at load bus [23].

Figure 8 illustrates the adjustment of two port equations for voltage level and drop with a solar PV power resulting in (5) and (6).

$$|V_2| = |V_1| - \frac{(R(P - P_{PV}) + XQ)}{|V_2|} \tag{5}$$

$$\Delta V = \frac{(R(P - P_{PV}) + XQ)}{|V_2|} \tag{6}$$

Equations (5) &(6) show that the voltage drop decreases proportionally with the increase in active power of PV therefore, the voltage at bus 2 would be increased.

IV. IMPACT AND INTEGRATION OF PV ON POWER LOSSES

As power is transported and distributed to the loads, as well as when major power plants are erected long distances from the supply and demand centres, there is often a significant amount of energy that is wasted in each of these processes. The conditions of each area influence the proportionality and distance of power loss that occurs when it travels over transmission lines. PV systems provide power at the points of consumption, and the amount of power produced is dependent on the amount of solar radiation that is available. These systems offer minimal power loss. There is no requirement for land because photovoltaic panels can be integrated into or mounted on the structure that requires electricity. As a consequence of this, the value that the PV system contributes to the grid is increased. If power is generated at the point of consumption, transmission and distribution losses decrease [23].

In (7) and (8) demonstrate the active and reactive losses

$$P_{Loss} = |I|^2 R = \left(\frac{P^2 + Q^2}{|V_2|^2} \right) R \tag{7}$$

$$Q_{Loss} = |I|^2 X = \left(\frac{P^2 + Q^2}{|V_2|^2} \right) X \tag{8}$$

Figure 8 depicts the change of two port equations for power losses consequential of the addition of solar PV power, as illustrated in (9) and (10).

$$P_{Loss} = |I|^2 R = \left(\frac{(P - P_{PV})^2 + Q^2}{|V_2|^2} \right) R \tag{9}$$

$$Q_{Loss} = |I|^2 X = \left(\frac{(P - P_{PV})^2 + Q^2}{|V_2|^2} \right) X \tag{10}$$

The penetration level of solar photovoltaic (PV) generation refers to the proportion or percentage of solar energy in the total electricity generation. It indicates how much of the total power demand is being met by solar PV sources. In other words, it measures the degree to which solar energy contributes to the overall energy supply within a particular region or system. Mathematically, the penetration level can be calculated as:

$$PV \text{ Penetration } (\%) = \frac{\text{Total PV generation (MW)}}{\text{Total generation (MW)}} \tag{11}$$

The total generation capacity in the IEEE 14-bus test system is 273 MW. A penetration level of 100 % means that all loads in the network are fed entirely by the distributed solar PV and a penetration level of 0 % means the grid entirely powers all the network loads. In this study, a penetration level starting from 10 % up to 100 % was used. After running the power flow to determine the most susceptible bus for photovoltaic (PV) injection, a penetration level of 10 % was started. If there is a decrease in the active power loss, another 10 % making a total of 20 % was used to determine the capacity of PV to be injected. This continues up to 100 %. However, if there is an increase in the active power loss, the next susceptible bus will be tested for PV injection. The same procedure applies as explained above for the penetration level in eq (11).

This continued until the grid hosting capacity which is the maximum amount of distributed photovoltaic (PV) that can be integrated into the grid without causing significant technical or operational issues is achieved. After the optimal location is determined an optimal load flow by Newton Raphson has been run to assure the exact value of the PV.

V. RESULTS AND DISCUSSION

The condensers on buses 3, 6, and 8 have been removed, and PV % size levels have been put at each bus in the IEEE-14 bus system, with losses determined after installation. The relationship between PV percentage penetration size and losses has been tabulated for each bus, and the relation curve was drawn.

The greatest and worst buses were selected. Therefore, the results obtained were as in the following table (I), and the accompanying graphic displays the results:

Table I: The relationship between the penetration and losses at bus 4.

penetration (%)	0	10	20	30	40	50	60	70	80	90	100
PV(MW)	0	27.3	54.6	81.9	109.2	136.5	163.8	191.1	218.4	245.7	273
losses (MW)	0	13.40	10.85	8.81	7.27	6.20	5.61	5.47	5.77	6.52	7.68

According to Table (I), which is shown visually in Figure (9), bus 4 has the best PV allocation, and the best PV penetration size level is 70%, resulting in fewer losses.

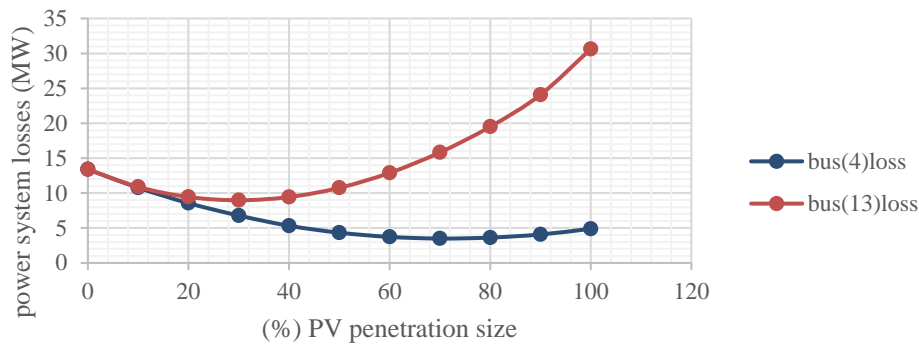


Figure 9 the relation between power losses and PV penetration.

Figure (9) shows the best bus allocation, bus 4, and the worst, bus 13.

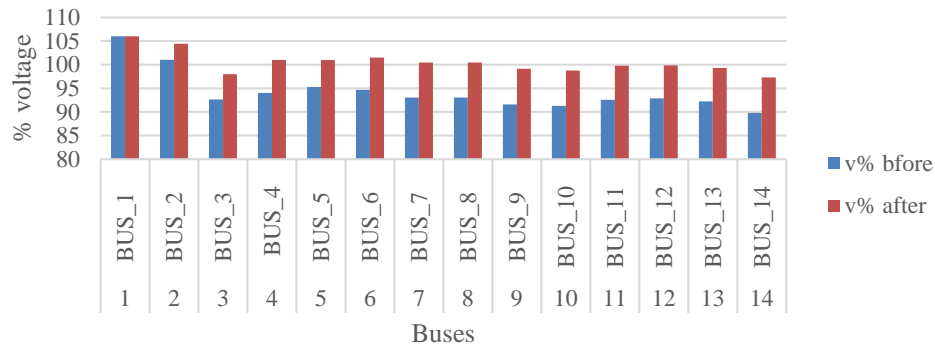


Figure 10 The voltage profile before and after installing PV source .

The voltage profile as illustrated in figure (10) has been improved at the entire system buses after installing the PV at 70% level, which is 191.1 MW as shown in table (I), taking into account the minor overvoltage at (bus1), which can be adjusted by running an optimal load flow to obtain an exact PV value of 185.87 MW, which represents 68% of the PV penetration level.

VI. CONCLUSION

This study defined the solar energy system, which consists of three main components: a solar panel, a power inverter, and a controller. The mathematical relationship connecting the solar energy unit to both network loss and electrical voltage was investigated and analysed. The influence of solar energy on the network was analysed assuming a power factor of one,

suggesting that the energy obtained from the solar energy unit is just reactive power. This study employed analytical and simulation techniques to find the best % penetration size and position for installing photovoltaic (PV) on the IEEE 14 bus system. The total generation capacity is 273 megawatts. In this investigation, penetration levels ranging from 10% to 100% were used. A power flow was run to determine the most vulnerable bus for photovoltaic (PV) injection, and a 10% penetration level was initiated. If the active power loss decreases, an additional 10%, for a total of 20%, is utilised to determine the PV injection capacity. This goes up to 100%. However, if the active power loss increases, the next susceptible bus will be examined for PV injection, resulting in the best penetration size of 191.1 MW, representing a 70% penetration rate. An ideal power calculation using the Newton Raphson technique was also performed to ensure the best results and the exact value of the optimal size, which is 185.87 MW (68%) and the optimal position at (bus 4).

REFERENCES

- [1] R. Shah, N. Mithulananthan, R. C. Bansal, and V. K. Ramachandaramurthy, 'A review of key power system stability challenges for large-scale PV integration', *Renew. Sustain. Energy Rev.*, vol. 41, pp. 1423–1436, 2015, Accessed: Aug. 11, 2024. [Online]. Available: <https://www.sciencedirect.com/science/article/pii/S1364032114008004>
- [2] A. J. Sangster, 'Solar Photovoltaics', in *Electromagnetic Foundations of Solar Radiation Collection*, in *Green Energy and Technology*, Cham: Springer International Publishing, 2014, pp. 145–172. doi: 10.1007/978-3-319-08512-8_7.
- [3] Y. He, Y. Pang, X. Li, and M. Zhang, 'Dynamic subsidy model of photovoltaic distributed generation in China', *Renew. Energy*, vol. 118, pp. 555–564, 2018, Accessed: Aug. 11, 2024. [Online]. Available: <https://www.sciencedirect.com/science/article/pii/S0960148117311436>
- [4] 'Renewable Energy in India - Indian Power Industry Investment'. Accessed: Sep. 09, 2024. [Online]. Available: <https://www.investindia.gov.in/sector/renewable-energy>
- [5] H. Alfrd, 'Optimal Power Loss Minimization using Optimal Size and Location of Shunt Capacitors, and DG', 2018, Accessed: Aug. 16, 2024. [Online]. Available: https://dSPACE.ELMergib.edu.ly/bitstream/handle/123456789/31/CEST_2_111.pdf?sequence=1&isAllowed=y
- [6] H. Alfrd and M. Khamaira, 'Voltage Stability Assessment and Improvement Index using Load Shedding and a Shunt Capacitor', *Elmergib J. Electr. Electron. Eng.* ISSN 2959-0450, vol. 1, no. 1, pp. 35–41, 2022, Accessed: Aug. 16, 2024. [Online]. Available: <https://ejeee.elmergib.edu.ly/index.php/ejeee/article/view/15>
- [7] M. M. Haque and P. Wolfs, 'A review of high PV penetrations in LV distribution networks: Present status, impacts and mitigation measures', *Renew. Sustain. Energy Rev.*, vol. 62, pp. 1195–1208, Sep. 2016, doi: 10.1016/j.rser.2016.04.025.
- [8] G. Guerra and J. A. Martinez, 'A Monte Carlo method for optimum placement of photovoltaic generation using a multicore computing environment', in *2014 IEEE PES General Meeting| Conference & Exposition, IEEE, 2014*, pp. 1–5. Accessed: Aug. 11, 2024. [Online]. Available: <https://ieeexplore.ieee.org/abstract/document/6939559/>
- [9] M. Zainuddin, T. P. Handayani, W. Sunanda, and F. E. P. Surusa, 'Transient stability assessment of large scale grid-connected photovoltaic on transmission system', in *2018 2nd International Conference on Green Energy and Applications (ICGEA), IEEE, 2018*, pp. 113–118. Accessed: Aug. 11, 2024. [Online]. Available: <https://ieeexplore.ieee.org/abstract/document/8356270/>
- [10] N. R. Bujal, A. E. Hasan, and M. Sulaiman, 'Analysis of voltage stability problems in power system', in *2014 4th International Conference on Engineering Technology and Technopreneuship (ICE2T), IEEE, 2014*, pp. 278–283. Accessed: Aug. 11, 2024. [Online]. Available: <https://ieeexplore.ieee.org/abstract/document/7006262/>
- [11] M. J. E. Alam, K. M. Muttaqi, and D. Sutanto, 'A comprehensive assessment tool for solar PV impacts on low voltage three phase distribution networks', in *2nd International Conference on the Developments in Renewable Energy Technology (ICDRET 2012), IEEE, 2012*, pp. 1–5. Accessed: Aug. 11, 2024. [Online]. Available: <https://ieeexplore.ieee.org/abstract/document/6153499/>
- [12] H. Sadeghian, M. H. Athari, and Z. Wang, 'Optimized solar photovoltaic generation in a real local distribution network', in *2017 IEEE Power & Energy Society Innovative Smart Grid Technologies Conference (ISGT), IEEE, 2017*, pp. 1–5. Accessed: Aug. 11, 2024. [Online]. Available: <https://ieeexplore.ieee.org/abstract/document/8086067/>
- [13] S. Liu, T. Bi, and Y. Liu, 'Theoretical analysis on the short-circuit current of inverter-interfaced renewable energy generators with fault-ride-through capability', *Sustainability*, vol. 10, no. 1, p. 44, 2017, Accessed: Aug. 11, 2024. [Online]. Available: <https://www.mdpi.com/2071-1050/10/1/44>
- [14] T. Aziz and N. Ketjoy, 'PV penetration limits in low voltage networks and voltage variations', *IEEE Access*, vol. 5, pp. 16784–16792, 2017, Accessed: Aug. 11, 2024. [Online]. Available: <https://ieeexplore.ieee.org/abstract/document/8022856/>
- [15] Q. Alsafasfeh, O. A. Saraereh, I. Khan, and S. Kim, 'Solar PV grid power flow analysis', *Sustainability*, vol. 11, no. 6, p. 1744, 2019, Accessed: Aug. 11, 2024. [Online]. Available: <https://www.mdpi.com/2071-1050/11/6/1744>
- [16] IEEE SCC 21 IEEE Standards Coordinating Committee 21 Fuel Cells, Photovoltaics, Dispersed Generation and Energy Storage | H2tools | Hydrogen Tools'. Accessed: Aug. 11, 2024. [Online]. Available: <https://h2tools.org/fuel-cell-codes-and-standards/ieee-scc-21-ieee-standards-coordinating-committee-21-fuel-cells>
- [17] R. VanOverstraeten and R. Mertens, 'Physics, technology and use of photovoltaics', 1986, Accessed: Aug. 11, 2024. [Online]. Available: <https://www.osti.gov/biblio/5663116>

- [18] M. Azzouzi, D. Popescu, and M. Bouchahdane, 'Modeling of electrical characteristics of photovoltaic cell considering single-diode model', *J. Clean Energy Technol.*, vol. 4, no. 6, pp. 414–420, 2016, Accessed: Aug. 11, 2024. [Online]. Available: <https://www.jocet.org/vol4/323-S011.pdf>
- [19] N. Mohan, T. M. Undeland, and W. P. Robbins, *Power electronics: converters, applications, and design*. John Wiley & sons, 2003.
- [20] J. H. Enslin, M. S. Wolf, D. B. Snyman, and W. Swiegers, 'Integrated photovoltaic maximum power point tracking converter', *IEEE Trans. Ind. Electron.*, vol. 44, no. 6, pp. 769–773, 1997, Accessed: Aug. 11, 2024. [Online]. Available: <https://ieeexplore.ieee.org/abstract/document/649937/>
- [21] C. Prapanavarat, *Investigation of photovoltaic inverters*. The University of Manchester (United Kingdom), 2000. Accessed: Aug. 11, 2024. [Online]. Available: <https://search.proquest.com/openview/1c70274984b0b2e37716b808457074f2/1?pq-origsite=gscholar&cbl=51922&diss=y>
- [22] E. Mulenga, 'Impacts of integrating solar PV power to an existing grid. Case Studies of Mölndal and Orust energy distribution (10/0.4 kV and 130/10 kV) grids.', 2015, Accessed: Aug. 11, 2024. [Online]. Available: <https://odr.chalmers.se/handle/20.500.12380/218826>
- [23] A. R. Alzyoud et al., 'The impact of integration of solar farms on the power losses, voltage profile and short circuit level in the distribution system', *Bull. Electr.Eng.Inform.*, vol.10,no.3,pp.1129–1141, 2021, Accessed: Aug. 11, 2024. [Online]. Available: <https://www.beej.org/index.php/EEI/article/view/1909>